J Mater Sci (2007) 42:10000–10006
DOI 10.1007/s10853-007-2050-7

Control of solidified structures in aluminum–silicon alloys by high magnetic fields

Qiang Wang · Chun-jiang Wang · Tie Liu · Kai Wang · Ji-cheng He

Received: 13 February 2006 / Accepted: 24 July 2007 / Published online: 6 September 2007

Abstract In order to investigate the effects of high magnetic fields on the as-solidified structures of Al alloys, solidification experiments of hypoeutectic and hypereutectic Al–Si alloys under various high magnetic field conditions (up to 12 T) have been conducted. It was found that uniform magnetic fields and gradient magnetic fields affect the solidification process by Lorentz force and magnetization force, respectively. The primary silicon crystals of hypereutectic Al–Si alloys are distributed, relatively, homogeneously under uniform magnetic fields, whereas they congregate near the top surface or bottom of samples by the combined action of buoyancy and magnetization force under gradient magnetic fields. The results indicate that it is possible to control the behaviors of reinforced particles in the metal matrix and improve the material performances by using high magnetic fields in the solidification process of metal matrix composites. The experiments also showed that high magnetic fields decrease the interlamellar spacing of the eutectic structure, while there exists a certain optimum value of magnetic intensity corresponding to the minimum value of interlamellar spacing, and magnetic energy is capable of influencing thermodynamic equilibrium of solidifying system and makes the content of eutectic aluminum in eutectic structures increased.

Q. Wang (✉) · C.-j. Wang · T. Liu · K. Wang · J.-c. He
Key Laboratory of Electromagnetic Processing of Materials (Ministry of Education), Northeastern University, Shenyang 110004, P.R. China
e-mail: wangq@mail.neu.edu.cn

Introduction

Electromagnetic processing of materials (EPM) has evolved as an important technique in the fields of material processing associated with shape controlling, flow driving, online detecting, heat generating, inclusion removing, magnetic levitation, and so on [1–5]. With advances in cryonetics and superconducting techniques, high magnetic fields became readily available in various scientific processes since 1980s, and with this trend, a new scientific research fields named "material processing by using a high magnetic field" came into being as a branch of EPM [6, 7]. Now, static high magnetic field facilities in some laboratories can generate high static field up to 45 T [8, 9].

Recently, an increasing number of studies have been focused on the control of solidification process under extreme conditions, which has been recognized as an effective way to improve material performances. High magnetic fields, as a promising technique, are helpful to create some new phenomena and discoveries, especially in solidification process. A high magnetic field enhances a Lorentz force, even with a weak electric current, and a magnetization force, which is tangible not only in ferromagnetic materials, but also nonmagnetic ones, such as paramagnetic and diamagnetic materials. Previous research on high magnetic fields conducted to help us to discover and explain phenomena have confirmed that the high magnetic field of 8 T can improve the quality of InGaSb crystal and the homogeneity of axial profile of Te impurity [10], and in the case of 10 T, it can promote or restrain nucleus formation and control dendrite crystal growth orientation [11]. Furthermore, ferromagnetic MnBi crystals in Bi–Mn alloy align and grow preferentially along the applied field and Al–7%Si–5%Fe intermetallic compound precipitated in a planar shape from an Al–11Si%–2%Fe

molten alloy aligns perpendicular to the magnetic fields [12, 13]. However, the integrative mechanism of Lorentz force and magnetization force acting on solidification process is not yet sufficiently understood, because of the experimental difficulty and the complexity of the phenomena.

The purpose of the present study is to qualitatively and quantitatively investigate the effects of uniform and gradient magnetic fields on the distribution of primary silicon crystals in eutectic matrix and the solidification process of eutectic reaction. Al–Si alloy has the advantage of broad application and appropriate magnetic properties. Meanwhile, hypereutectic Al-Si alloy can also be considered as in situ metal matrix composites, in which the primary silicon crystals are treated as reinforcement particles distributed in the matrix of Al–Si eutectic. For that reason, this kind of alloy was selected for the experiments. High magnetic fields of different intensities and gradients have been imposed on three different Al–Si alloys during melting and solidification, and the results have been analyzed and discussed.

Experiments

Preparation of Al–Si alloys

Commercially pure aluminum and 99.99% silicon with given mass percent were heated in graphite crucible to 900 °C and held for 1 h to make sure the mixture fully melted. The molten alloy was stirred for 5 min to ensure the complete homogeneity during cooling to 800 °C. Finally, the graphite crucible was removed from the furnace and the molten alloy was poured into a chilled mould. Three Al–Si alloys were prepared and analyzed: Al–15.7 wt.%Si, Al–15.0 wt.%Si, and Al–9.2 wt.%Si. The as-solidified alloys were then cut into rod specimens (9 mm in diameter, 30 mm in height) for the solidification experiments under magnetic field conditions.

Solidification experiments in uniform high magnetic fields

Figure 1 shows the schematic view of the experimental apparatus and the characteristics of the superconducting magnet. The uniform magnetic fields could only be obtained at the position of B_{max} according to Fig. 1b, and the magnetic flux density in B_{max} position could be controlled between 0 T and 12 T, three values of magnetic flux density B, 0 T, 6 T, and 12 T were selected in this experiment. A resistance furnace was used to heat and melt the sample, whose temperature could be regulated by an

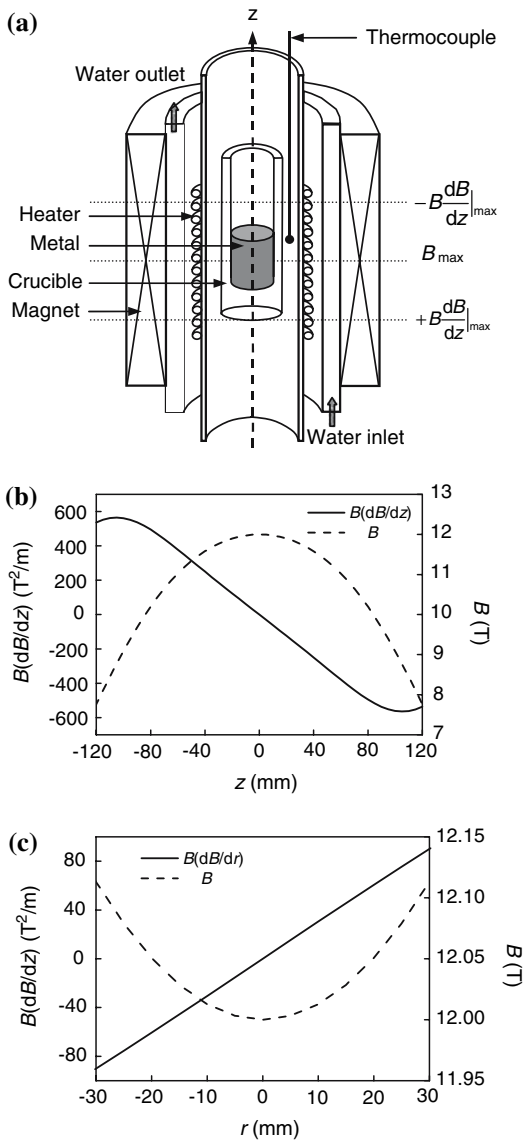

Fig. 1 Schematic illustration of experimental apparatus (**a**) and the characteristics of the magnet in the axial direction (**b**) and radial direction (**c**) at B_{max} = 12 T

R-type thermocouple set in the center of the furnace. A cylindrical specimen was put into an alumina crucible of 10 mm in diameter and then was fixed in the position B_{max} inside the bore of super-conducting magnet. The uniformity of the field over the dimensions of the sample can be seen from Fig. 1c. Thereafter the sample was heated to 750 °C within 150 min and held at the same temperature for 10 min to make it completely melted. Finally, it was cooled down to room temperature at the rate of about 15 °C min^{-1}. All the operations were performed in vacuum to void pollution. After cutting longitudinally the treated samples and grinding and polishing, the macro- and microstructures of the solidified specimens were observed by an optical microscope.

Solidification experiments under gradient high magnetic fields

Experimental apparatus and temperature curve were both same as the cases of uniform fields mentioned above. In order to give prominence of the effects of magnetic gradient, two positions were chosen such as the plus and minus maximum product of magnetic flux density and its gradient $\pm B(\mathrm{d}B/\mathrm{d}z)_{\max}$ based on Fig. 1b. The absolute value of product $|B(\mathrm{d}B/\mathrm{d}z)|$ could be controlled between 0 T^2 m^{-1} and 564 T^2 m^{-1}. The chosen product of $B(\mathrm{d}B/\mathrm{d}z)$ and corresponding B in this study were $\pm$ 564 T^2 m^{-1}, and 8.8 T, respectively. The employment of these two utmost positions which were both located at the edge of the chamber of resistance furnace would bring some effects on the solidified structures, and it will be discussed in details below.

Results and discussion

The effects of magnetic intensity on solidified structures

Figure 2 shows solidified macrostructures of Al–15.7 wt.%Si specimens treated under various magnetic field conditions. Figure 2a presents the macrostructures of the specimens imposed by the magnetic field of 0 T. Primary silicon crystals were mainly observed at the bottom and the edge of the sample and few of them were observed at the center region in the sample. This resulted from the solidification direction of the sample caused by the fact that it was contacting with the wall of crucible. In contrast, when the specimen was subjected to the magnetic fields, the distribution of primary silicon crystals changed remarkably and the primary silicon crystals appeared at the middle and the upper regions in the samples as well as the bottom and the edge, as shown in Fig. 2b and c. Furthermore, the fraction of the primary crystals increased with the increasing intensity of magnetic fields. All these indicated that the introduction of the magnetic fields changed the solidification conditions of the melted alloy and influenced the solidification processes evidently. That is, Lorentz force caused by magnetic fields strongly suppressed the convection of the melted alloy [14, 15] so as to weaken the mass transport of solute and the migratory behavior of primary silicon crystals. In this case, it can be concluded that uniform magnetic fields can make the primary silicon crystals distribute rather uniformly during the solidification processes of Al–Si hypereutectic alloy, and consequently, it can be adopted to the technique of fabricating in situ metal matrix composites. It can be clearly found that the distribution of hole, which is generated by the aggregated bubbles of gas dissolved in the melt, is also changed. In Fig. 2a, the hole is located in the upper part of the specimen, whereas it is moved to the center in the cases of the magnetic field. The bubbles can easily float up and aggregate together in the upper part of the specimen because of the density difference between the bubble and the melt, whereas, it would be relatively difficult for the bubbles to float and aggregate in the presence of magnetic fields due to the braking effect of Lorentz force on the convection. Based on the similar braking effect between Lorentz force and viscous resistance, the braking effect of Lorentz force can be evaluate quantitatively by using effective viscosity η_{eff} under magnetic field, which is relating to Hartman number Ha [16]:

$$\eta_{\mathrm{eff}} = \eta \frac{Ha}{3} \tag{1}$$

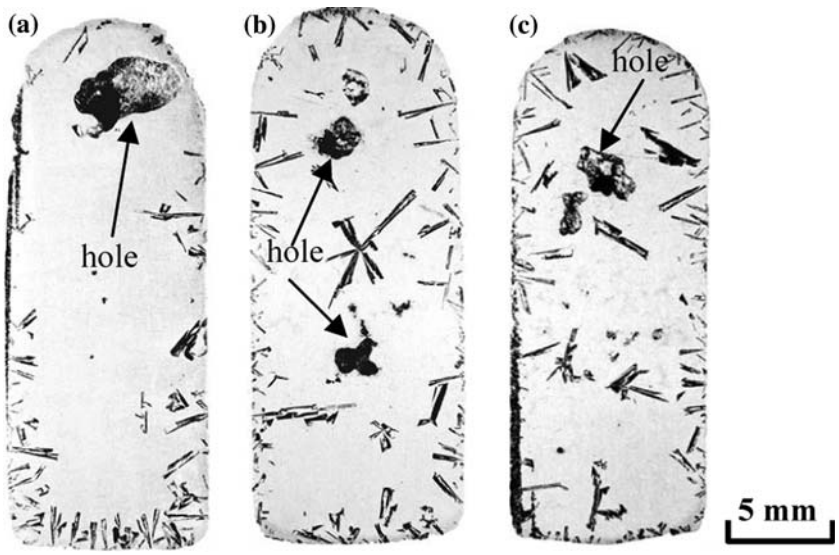

Fig. 2 Macrostructures of Al–15.7 wt.%Si alloy under various magnetic field conditions. (**a**) 0 T, (**b**) 6 T, (**c**) 12 T

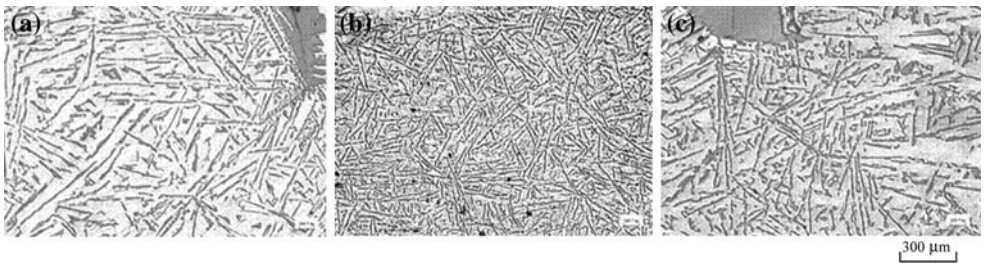

Fig. 3 Microstructures of Al–15.7 wt.%Si alloy under various magnetic field conditions. (**a**) 0 T, (**b**) 6 T, (**c**) 12 T

where, η is the viscosity without magnetic field, $Ha = Bl\sqrt{\frac{\sigma_m}{\eta}}$, l is characteristic length and σ_m is the electrical conductivity of the melt. For the metal with a characteristic length of 10^{-5} m under a magnetic field of several Tesla in the present study, η_{eff} is larger than η because Ha is significantly larger than 10.

In Fig. 3, the microstructures of Al–15.7 wt.%Si alloy under various magnetic fields, 0 T, 6 T, and12 T, all present typical fibrous Al–Si eutectic structures, which is the morphology in most solidification processes. It is obvious that the eutectic structures are refined at 6 T. This phenomenon, however, is not quite noticeable in the case of 12 T. It actually implies that there is an optimum value of magnetic fields, which can bring the minimum of interlamellar spacing. Although the mechanism is not very clear yet, it can be conjectured that the improvement of nucleation rate [17], which makes a key contribution to refining eutectic structures, is the dominant factor below the optimum value. However, the suppression of the thermal convection becomes the dominant factor that is in favor of enhancing crystals growth with the increasing of magnetic fields above the optimum value.

The effects of magnetic field gradients on solidified structures

Figure 4 shows the effects of magnetic gradients on the distribution of primary silicon crystals of Al–15.0 wt.%Si alloy at 0 T and $B_{\max}$ position, 8.8 T with $B(\mathrm{d}B/\mathrm{d}z)$ = 564 T^2 m^{-1}, 8.8 T with $B(\mathrm{d}B/\mathrm{d}z)$ = –564 T^2 m^{-1} and 0 T and $-B(\mathrm{d}B/\mathrm{d}z)_{\max}$ position, respectively. Comparing Fig. 4b, and c with a, it can be found that the distribution of silicon crystals has been changed remarkably. When it is under gradient magnetic field conditions, the silicon crystals aggregate at upper part or lower part of the sample, while the primary silicon crystals appear only at the edge of the samples without magnetic field. Furthermore, other experiments confirmed that this phenomena became more obvious with the increasing of the product of magnetic flux densities and magnetic gradients ($B(\mathrm{d}B/\mathrm{d}z)$) [18].

Due to small difference in density between silicon-crystal and aluminum-melt, the primary silicon crystals segregate where solidification takes place initially. Thus, the above-mentioned phenomena may result from different solidification directions at the positions of $B_{\max}$ = 0, $B(\mathrm{d}B/\mathrm{d}z)_{\max}$, and $-B(\mathrm{d}B/\mathrm{d}z)_{\max}$. If it is just the

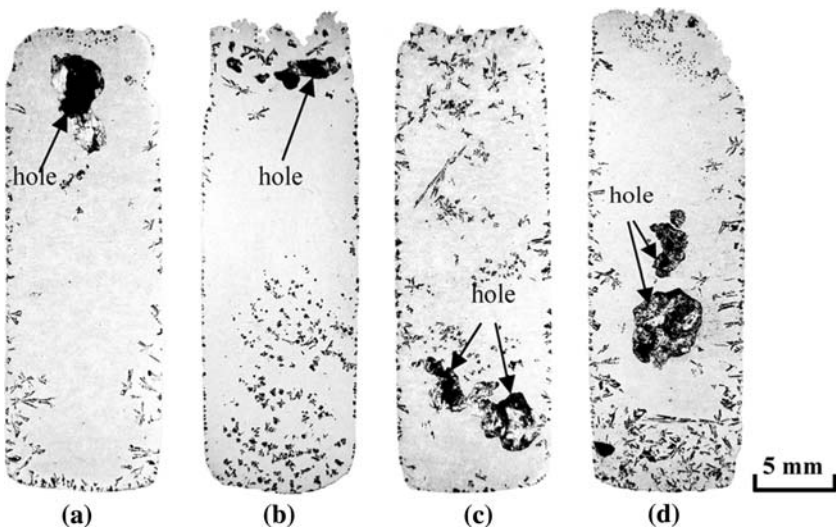

Fig. 4 Macrostructures of Al–15.0 wt.%Si alloy under various gradient magnetic field conditions. (**a**) 0 T, $B_{\max}$ position; (**b**) 8.8 T, $B(\mathrm{d}B/\mathrm{d}z)_{\max}$ = 564 T^2 m^{-1}; (**c**) 8.8 T, $B(\mathrm{d}B/\mathrm{d}z)_{\max}$ = –564 T^2 m^{-1}; (**d**) 0 T, $-B(\mathrm{d}B/\mathrm{d}z)_{\max}$ position

case, the distributions of primary silicon crystals in Fig. 4c and d should be similar because these two samples have same temperature profiles during the solidification processes. Experimental results show, however, that primary silicon crystals segregate in the edge of the sample without magnetic fields and in the upper part of the sample with magnetic fields. Considering the contravention, there must be other factors that effect the distribution of primary silicon crystals.

For nonmagnetic aluminum and silicon, the magnetization force caused by high gradient magnetic fields is enhanced so largely that it cannot be ignored at all. When the alloy solidified under gradient magnetic fields, the primary silicon crystals and Al–Si eutectic matrix are subjected to the action of magnetization force and gravity. Since silicon crystals are generated in aluminum melts, the effects of aluminum medium must be taken into account. The resultant force F acting on primary silicon crystals is given by Eq. (2) in the assumption that crystals are not moving and so only the driving forces are considered [19].

$$F = -(1/\mu_0)(\chi_{\mathrm{Al}} - \chi_{\mathrm{Si}})B(\mathrm{d}B/dz) + (\rho_{\mathrm{Al}} - \rho_{\mathrm{Si}})g \qquad (2)$$

where μ_0, χ, ρ, and g are vacuum permeability, volumetric magnetic susceptibility, density, and gravitational acceleration, respectively. The physical properties of Al and Si are $\rho_{\mathrm{Al}} = 2360$ kg m^{-3}, $\rho_{\mathrm{Si}} = 2520$ kg m^{-3} [20], $\chi_{\mathrm{Al}} = 1.94 \times 10^{-5}$, and $\chi_{\mathrm{Si}} = -0.91 \times 10^{-5}$ [21]. In the case of $B(\mathrm{d}B/\mathrm{d}z) = 0$, namely without magnetic fields or with uniform magnetic fields, Eq. (2) can be rewritten as $F = (\rho_{\mathrm{Al}} - \rho_{\mathrm{Si}})g$, as a result, the crystals will move downwards due to $F < 0$ in the condition $\rho_{\mathrm{Al}} < \rho_{\mathrm{Si}}$. In this experiment, the phenomena were not very distinct since the density difference between aluminum and silicon was rather small. If Eq. (2) meets the case of $B(\mathrm{d}B/\mathrm{d}z) \neq 0$ and $F = 0$, it means that the magnetization forces reach equilibrium with the gravity, silicon crystals will levitate freely in the metal, and this case can be used to suppress macro segregation or improve homogeneous distribution. When $B(\mathrm{d}B/\mathrm{d}z) \neq 0$ and $F \neq 0$, the crystals will aggregate at the certain side of the sample according to the direction of F.

According to the analysis above, the behavior of silicon crystal is dominated by the resultant forces acting on it. In the case of $B(\mathrm{d}B/\mathrm{d}z) = 564$ T^2 m^{-1} and $B(\mathrm{d}B/\mathrm{d}z) = -564$ T^2 m^{-1}, the resultant force $F \approx -8000$ N m^3 and $F \approx 15000$ N m^3, respectively. The silicon crystal begins to take accelerating movements due to the force F, and viscosity resistance acting on the silicon crystal increases simultaneously with the velocity. Besides, the Lorentz force, induced by the movement of the metal under magnetic field condition, should be considered. Generally, Lorentz force will also counteract the motion of crystals in the solidification process and make the crystals slow down gradually. The primary silicon crystals achieve a force balance and begin to have a uniform motion when the velocity increases to a terminal value v_{f}

$$v_f = \frac{2}{9}\frac{Fr^2}{\eta_{\mathrm{eff}}} \qquad (3)$$

where r is the radius of silicon crystal, which is assumed to be spherical. For silicon crystal with radius $r = 0.05$ mm and magnetic field $B = 8.8$ T, the terminal value $v_{\mathrm{f}} \approx 2$ mm s^{-1}. It is obvious that magnetization force dominates the movement of primary silicon crystals under gradient high magnetic fields, and the experimental results that most of silicon particles appear at the bottom or top of samples, as shown in Fig. 4b and c, are accordant with the theoretical analysis above. On the other hand, there also are a fair amount of primary silicon crystals on the sides of the samples. This is because of the solidification direction of the sample caused by the fact that it was contacting with the wall of crucible.

The effects of magnetic energy on solidified structures

Comparing Fig. 2a with Fig. 2b and c and Fig. 4a and d with Fig. 4b and c, the fact that the volume fraction of primary silicon crystals increases with magnetic flux intensity can be clearly observed. So it can be concluded that magnetic fields can promote the separation of silicon out of Al–Si alloy. The mechanism by which high magnetic fields affect the solidification process thermodynamically and dynamically must be discovered in order to explain the observation that the volume fraction of primary silicon crystals increases. The fact that high magnetic fields suppress convection of the melted alloy contributes to slow down the solidification process because of the decrease in heat dissipation speed and it allows primary silicon crystals enough time to nucleate and grow up. It has been known that high magnetic fields can affect the energy of solidified system since magnetic fields can transfer contactlessly magnetic energy into materials, especially in the process of phase transformation. The effect of magnetic energy on solidification system during eutectic reaction is discussed in details as follows.

The Al–Si alloy with eutectic composition is treated as the solidified system. Then the magnetic energy of eutectic aluminum ($\mathrm{Al_{eu}}$) and eutectic silicon can be expressed as W_{mAl} and W_{mSi}, respectively. Magnetic energy is given by $W_{\mathrm{m}} = \frac{1}{2}\frac{B^2}{\mu}$, where μ is the absolute magnetic permeability and $\mu = (1 + \chi)\mu_0$. So the difference of magnetic energy between eutectic silicon and eutectic aluminum can be expressed as

$$\Delta W_m = W_{mSi} - W_{mAl} = \frac{B^2}{2}\left(\frac{1}{\mu_{Si}} - \frac{1}{\mu_{Al}}\right) = \frac{B^2}{2\mu_{Si}\mu_{Al}}(\mu_{Al} - \mu_{Si}) = \frac{\mu_0 B^2}{2\mu_{Si}\mu_{Al}}(\chi_{Al} - \chi_{Si}) \quad (4)$$

It is obvious that $\Delta W_m > 0$ in Eq. (2) because of $\chi_{Al} > \chi_{Si}$, so the increase of relative volume fraction of eutectic aluminum in eutectic will contribute to reduce systematic magnetic energy and stabilize the system. Hence, more eutectic aluminum is crystallized during eutectic reaction under magnetic fields.

Based on the analysis above, the solidification process of hypereutectic Al–Si alloy under magnetic fields can be described as follows: The primary silicon crystals separate initially as soon as solidification starts. With the temperature of the remaining melt decreases, the melt composition reaches the eutectic one and an invariant eutectic reaction occurs. During the solidification process, both the thermodynamics and dynamics factors induced by the imposed magnetic fields contribute to the increase of primary silicon crystals.

In order to confirm the results of experiments on hypereutectic Al–Si alloy, solidification experiments on Al–9.2 wt.%Si hypoeutectic alloy were also conducted under magnetic field conditions of 0 T and 12 T, respectively. The structures of Al–9.2 wt.%Si hypoeutectic alloy consisted of primary aluminum(α) and Al–Si eutectic. Quantitative volume analysis of the microstructures was taken in present study by using SISCIA software and the mass content of β_{II} (Si) in α was measured by an electron microprobe (Fig. 5). Fig. 5 shows that the content of primary aluminum(α) remains approximately constant while the contend of Al_{eu} in eutectic and β_{II} (Si) in primary aluminum(α) increases with increasing magnetic flux intensity, in agreement with the conclusions obtained from the experiments on hypereutectic system.

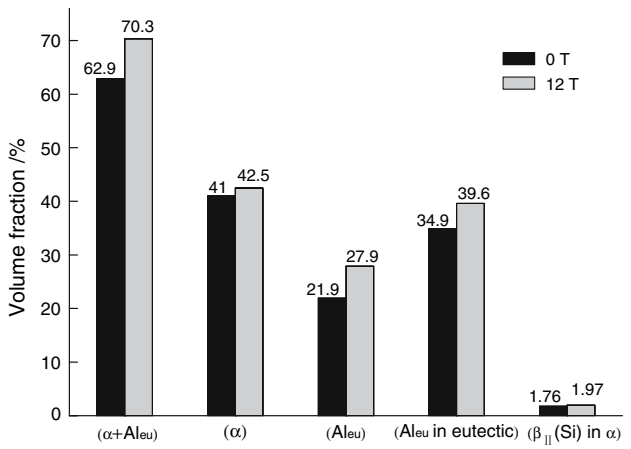

Fig. 5 Contents of phases in Al–9.2 wt.%Si specimens at 0 T and 12 T

Conclusions

Effects of high magnetic fields on the distribution of the primary crystals and the solidification structures of eutectic (in Al–Si alloy) were investigated. It was found that Lorentz force, magnetization force, and magnetic energy, all had great effects on solidification processes, and the following results were obtained:

(1) The primary Si crystals are distributed relatively homogeneously, especially in the magnetic direction, and the interlamellar spacing of eutectic structures decreases under uniform magnetic fields with an optimum value of magnetic intensity corresponding to the minimum of interlamellar spacing.
(2) Magnetization force induced by magnetic gradient dominates the distribution of primary Si crystals in hypereutectic Al–Si alloy, and so gradient magnetic fields can be used to control the distribution of reinforcement particles in metal matrix composites. The reinforcement particles can be distributed homogenously or aggregated in a certain side for different purposes under different magnetic field conditions.
(3) The amount of eutectic aluminum increases during eutectic reaction of Al-Si alloy due to the effects of magnetic energy.

Acknowledgement This work was supported by the National Natural Science Foundation of China (Grant No. 50374027), the Program for New Century Excellent Talents in University (Grant No. NCET-06-0289) and the 111 project (Grant No. B07015).

References

1. Asai S (2003) In: Asai S, Fautrelle Y, Gillon P, Durand F (eds) Proceedings of the 4th International Conference on Electromagnetic Processing of Materials, Lyon, The Company Forum Edition, Lyon, p 1
2. Asai S (2000) Sci Technol Adv Mater 1:191
3. Jones TB (1979) J Appl Phys 50:5057
4. Garcia A, Moron C, Maganto F (2003) Sensor Actuat A-Phys 106:108
5. Negrini F, Fabbri M, Zuccarini M, Takeuchi E (2000) Energy Convers Manage 41:1687
6. Asai S (2004) Model Simul Mater Sci Eng 12:R1
7. Asai S, Sassa K, Tahashi M (2003) Sci Technol Adv Mater 4:455
8. Schneider-Muntau HJ, Brandt BL, Brunel LC, Cross TA, Edison AS, Marshall AG, Reyes AP (2004) Physica B 346–347:643
9. Perenboom JAAJ, Wiegers SAJ, Christianen PCM, Zeitler U, Maan JC (2004) Physica B 346–347:659
10. Kang JY, Tozawa S (1996) Acta Phys Sin 45:324
11. Wang Q, Wang CJ, Wang EG, He JC (2005) Acta Metall Sin (in Chinese) 41:128
12. Wang H, Ren ZM, Deng K, Xu KD (2002) Acta Metall Sin (in Chinese) 38:41
13. Morikawa H, Sassa K, Asai S (1998) Mater Trans JIM 39:814
14. Yasuda H, Ohnaka I, Ninomiya Y, Ishii R, Fujita S, Kishio K (2003) In: Asai S, Fautrelle Y, Gillon P, Durand F (eds)

Proceedings of the 4th International Conference on Electromagnetic Processing of Materials, Lyon, The Company Forum Edition, Lyon, p 459
15. Nakada M, Mori K, Nishioka S, Tsutsimi H (1997) ISIJ Int 37:358
16. Yasuda H, Ohnaka I, Kawakami O, Ueno K, Kishio K (2003) ISIJ Int 43:942
17. Wang Q, Wang EG, He JC, Hu K, Takahashi K, Watanabe K (2003) In Asai S, Fautrelle Y, Gillon P, Durand F (eds) Proceedings of the 4th International Conference on Electromagnetic Processing of Materials, Lyon, The Company Forum Edition, Lyon, p 464
18. Wang Q, Wang CJ, Pang XJ, He JC (2004) Chinese J Mater Res (in Chinese) 18:568
19. Ikezoe Y, Kaihatsu T, Uetake H, Hirota N, Nakagawa J, Kitazana K (2000) Trans Mater Res Soc Jpn 25:77
20. Robert C (1982–1983) In: CRC Handbook of Chemistry and Physics (the 63rd edition), CRC Press, Inc., Florida, p B-244
21. The Japan Institute of Metals (1993) In: Data handbook of metals (the Third Edition, in Japanese), Maruzen Co. Ltd, Shizuoka, p 18